Review

Dan Aoki*, Yasuyuki Matsushita and Kazuhiko Fukushima

Cryo secondary ion mass spectrometry for wood component visualization: a mini review

https://doi.org/10.1515/hf-2021-0142
Received July 25, 2021; accepted October 20, 2021;
published online December 7, 2021

Abstract: Various phenomena in living physiological systems are conducted on the hydrated conditions, and in many cases, they do not work in a dry state. Imaging mass spectrometry is one of the direct detection methods scanning the sample surface with some focused and pulsed energy and analysing the sputtered components. However, under the high vacuum conditions required for usual imaging mass spectrometry, the sample surface is rapidly dried. It is difficult for the target cell to survive, and the original situation are lost soon. Here, the combination of a freeze-fixation and a cryo sample stage is a promising method to do mass spectrometry while maintaining the original situation. By rapidly freezing the cells, the momentary situation as a living cell is fixed. The situation in a living cell can be captured as still images by cryo imaging mass spectrometry. This mini-review introduces the outline of imaging mass spectrometry especially for low molecular weight components and recent results for frozen-hydrated samples by cryo secondary ion mass spectrometry.

Keywords: chemical mapping; cryo-TOF-SIMS; distribution; frozen-hydrated; imaging.

1 Introduction

Chemical visualization is a powerful approach to combine the chemical properties of the target compounds and their actual roles with their positional information in the system. There are several "microscopic" techniques using various detection principles such as micro-spectroscopy (IR, Raman, X-ray, fluorescence, radiation, colouration, etc.), imaging mass spectrometry, and also any analysis with micro sampling techniques.

In imaging mass spectrometry, focused ionisation energy is applied onto the sample surface, and the resultant charged particles of ions produced by the surface are detected. The ions receive kinetic energy from the electrodes and travel to the detector of time-of-flight (TOF), quadrupole, sector, or ion-trap types, etc. The obtained signal is displayed with the parameter mass-to-charge ratio (m/z), the mass of the ion divided by the number of charges, e.g., 26.98 for Al^+ and 13.49 for Al^{2+}. By repeatedly irradiating a small area with a focused and pulsed energy and performing detection, a mass spectrum can be obtained for each point, which is then used as a data per an imaging pixel. Therefore, the imaging mass spectrometry data set means an aggregate of mass spectra.

At the present time, the most versatile imaging mass spectrometers are probably matrix-assisted laser desorption/ionisation mass spectrometry (MALDI-MS), desorption electrospray ionisation mass spectrometry (DESI-MS), and secondary ion mass spectrometry (SIMS), which use a laser, a solvent electrospray, and a primary ion beam, respectively. Depending on their ionisation principles, their analytical characters such as spatial resolution, detection mass range, analytical throughput, MS^n applicability, and compound specific sensitivities are different. Briefly, MALDI-MS can detect large mass components but has low spatial resolution, and SIMS has high spatial resolution although it is limited to small mass components. SIMS can be classified to two major types; static-SIMS to measure molecules with TOF-detector, and dynamic-SIMS to measure elements with sector- or quadrupole-detectors. TOF-SIMS can measure only the top surface of a few nanometres depth owing to the minute irradiation power, and is called as static. DESI-MS is a relatively new technique enables measurements under ambient conditions without surface pre-treatments. The differences

***Corresponding author: Dan Aoki**, Graduate School of Bioagricultural Sciences, Nagoya University, Nagoya 464-8601, Japan, E-mail: aoki.dan@nagoya-u.jp.
https://orcid.org/0000-0003-3696-4103
Yasuyuki Matsushita, Institute of Agriculture, Tokyo University of Agriculture and Technology, Tokyo 183-8509, Japan.
https://orcid.org/0000-0003-1357-3927
Kazuhiko Fukushima, Graduate School of Bioagricultural Sciences, Nagoya University, Nagoya 464-8601, Japan

within these techniques are well described in elsewhere (Vickerman 2011).

There are many notable research using above introduced imaging mass spectrometry in the field of biomass chemistry, here the authors focus TOF-SIMS for wood component visualization with higher spatial resolution to some extent. The outline of TOF-SIMS measurement as mentioned above is schematically illustrated in Figure 1a. The fundamental aspects for SIMS are summarised in some treatises (Delcorte 2001; Hagenhoff 2001; Van der Heide 2014a; Vickerman 2001) and not introduced in detail here. The image size is variable and 256×256 pixels are often used. The images can be generated arbitrarily from the measurement RAW data, e.g., for total ion, for specific ion, and also for arithmetically processed values using the ion counts in the data matrix such as sum, subtraction, ratio, etc. In SIMS measurements, compared with MALDI and DESI, the target molecule [M] tends to be degraded and produces many fragment ions as suggested in Figure 1b. At the same time, the target molecule can be an adduct ion of $[M+X]^+$. Regarding the lower desorption/ionisation power of SIMS, it is hard to detect large molecules (Piwowar and Vickerman 2010) and major signals in TOF-SIMS spectra are fragment ions arisen from macromolecules such as cellulose and lignin (Goacher et al. 2011; Saito et al. 2005a, 2005b, 2006). Therefore, the important target compounds with TOF-SIMS should be macromolecules producing some characteristic fragment ions and also *as-is* detectable small molecules.

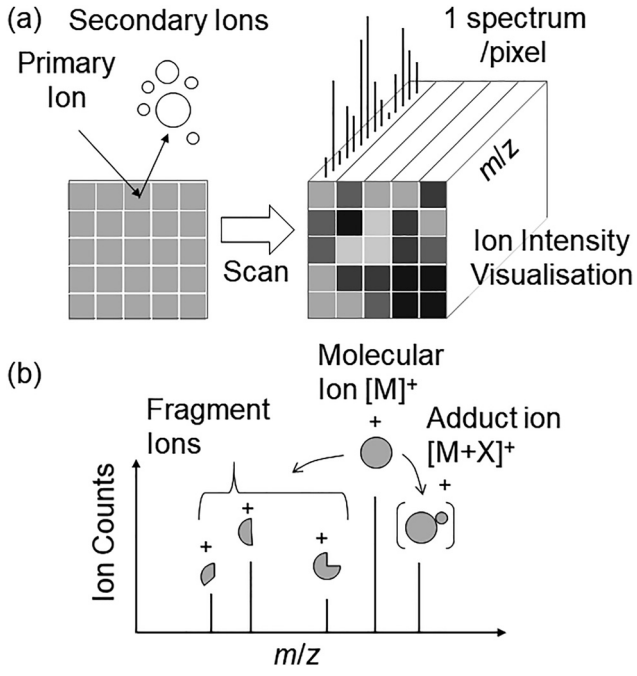

Figure 1: Schematic illustrations of (a) TOF-SIMS measurements and (b) secondary ion production.

2 Sample conditions

In mass spectrometry as well as in many other visualization techniques, one of the most important points is whether the resultant distribution is native or not. In other words, even if some meaningful distribution is obtained as a result of the analysis, the possibility should be in mind that such a distribution was not truly *in vivo*, but was artificially given in the sample preparation or analysis pre-treatment steps. Dealing with plant samples, for example, the major polymer components of cellulose, hemicellulose, and lignin anchored to each other can be detected without microscale positional denaturation. All of mobile components should be discussed carefully with this viewpoint if you would like to discuss their microscale distribution *in vivo* (Figure 2a).

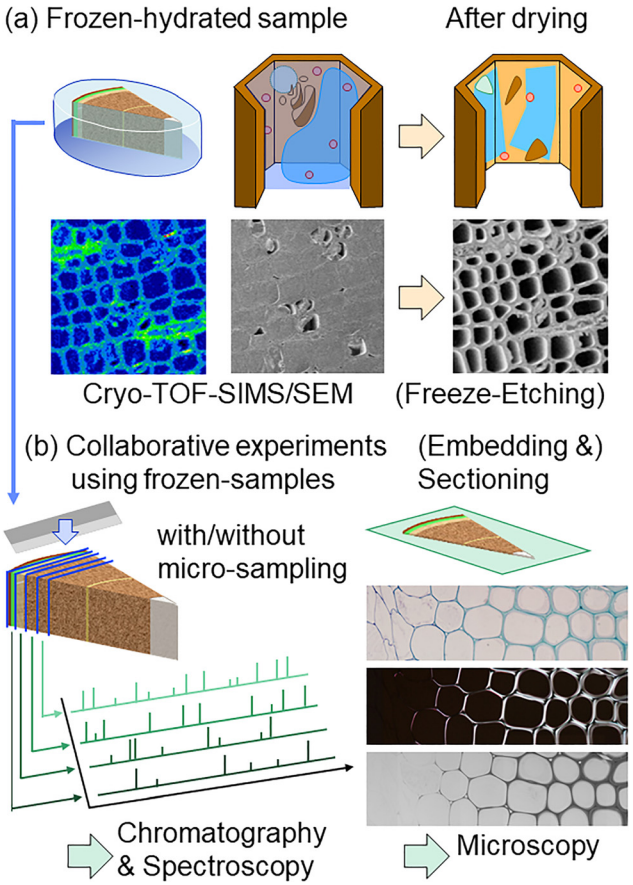

Figure 2: Schematic illustrations of (a) frozen-hydrated samples losing the precise positional information of the mobile components after drying, and (b) collaborative experiments of chromatography and spectroscopy to identify and quantify the target compounds, and microscopic observations to determine the cell and tissue types and their differentiation stages.

This issue has been discussed for a long time, especially in the field of microscopy, where freeze-fixation has played a major role in correctly viewing the shape of cell and its contents (Lancelle et al. 1986; Samuels et al. 2002). The preparation of sections from freeze-fixed samples, which is an important technique in microscopy, is also a basic sample preparation method in imaging mass spectrometry, but the sections are usually dried before analysis. However, artefacts such as a deformation of soft and fragile microstructures and a degradation or a diffusion of the contents, which are certain to occur as a result of the transition from a freeze-fixed to a dried state, are important issues in recent high spatial resolution imaging techniques.

In the field of imaging mass spectrometry, attempts to analyse freeze-fixed samples as intact as possible have been investigated. In fact, cryo sample stages for SIMS apparatus were developed at about the same time as the introduction of rapid freezing to the field of electron microscopy (Bernius et al. 1985; Chandra et al. 1986). However, until recently, there have been very few reports of cryo-TOF-SIMS analysis using frozen samples, especially for organic compounds. The major difficulty should be originated from the measurement principles of TOF-SIMS. TOF-SIMS needs high vacuum conditions, long measurement time, and measures only a few nanometres top surface; therefore, the frozen samples have to be treated without any surface contamination, frost deposition, or sublimation within the periods of the surface pretreatment, the introduction to the vacuum apparatus, and the measurement. A few research groups overcame this problem and reported the cryo-TOF-SIMS measurements for frozen-hydrated biological samples earlier (Cannon et al. 2000; Cliff et al. 2003; Colliver et al. 1997; Möller et al. 2006; Pacholski et al. 1998). Recently the cryo sample transfer techniques and cryo sample stages with an accurate temperature control are gradually distributed and further developments have been expected for cryo-TOF-SIMS measurements (Kuroda et al. 2013; Metzner et al. 2008; Newell et al. 2019; Phan et al. 2014; Piehowski et al. 2008; Piwowar et al. 2009; Sämfors et al. 2019; Tyler et al. 2006; Yoon and Lee 2018; Zhang et al. 2020).

3 Collaborative experiments with SIMS

Before going to the actual imaging data exhibitions, the authors suggest the collaborative experiments to enhance the TOF-SIMS applicability. TOF-SIMS measurement needs several supporting information about the target chemical identification, quantification, and tissue assignments to discuss their detailed distributions and possible roles in the system. Schematic illustration of the frozen-sample usage for chromatography, spectroscopy, and microscopy is shown in Figure 2b.

Compound identifications are essential process in chemistry. Although the latest SIMS apparatus can operate tandem (Fisher et al. 2016) and very high mass resolution (Passarelli et al. 2017) measurements, many research groups use LC, GC, NMR, IR, Raman, or any other characterization analyses to confirm the target compounds and compare the results with the previous reports. The quantitativity is also an inevitable issue in TOF-SIMS measurements and these supporting measurements work properly. Further, when these measurements are combined with the micro-sampling techniques, the resultant data is a kind of chemical mappings and supports TOF-SIMS images well; nevertheless, the experimental throughput should be considered.

On the other hand, TOF-SIMS data often collaborate with other microscopy images. Higher magnification for morphology, specific wavelength, polarization, fluorescence, conventional staining for cell and tissue type characterization, and combination of these techniques are so helpful to determine the cell and tissue classification within various differentiating stages. These observation techniques are widely used and their procedures are well established; however, it should be pointed that it is not easy to apply these observations on the same sample surface measured by TOF-SIMS.

4 Cryo-TOF-SIMS visualizations of wood relating components

In this mini review, the authors focus the cryo-TOF-SIMS application to wood and biomass samples to visualize the mobile components such as inorganic elements, small saccharides, glycosylated compounds and their aglycons, ionic compounds and a complex, and artificial additives and tracers to discuss aqueous reaction systems. These target compounds are annotated from the viewpoint of detection sensitivity, ionisation behaviour, and *in planta* distributions considering with their co-existing compounds.

Polymer components are not mentioned in this mini-review because their fragment ions are seldom detected in cryo-TOF-SIMS measurements. The authors surmise that the situation of the frozen-hydrated state containing much amount of water and under low temperature may disperse

the primary ion bombardment energy and prevent the polymer components from their fragmentation.

4.1 Inorganics

In plants, the order of the average contents of inorganic elements is reported as N > K > Ca > Mg, P, S > Cl, B, Fe, Mn, Zn, Cu, and others (Kirkby 2012). Here, alkaline metal of K is one of the most important elements owing to its abundance, high ionisation efficiency, and adducting ability to other particles (producing adduct ion as shown in Figure 1b). In TOF-SIMS, the ionisation efficiency can vary several orders of magnitude depending on their chemical character and the "matrix effect", which is a specific term in TOF-SIMS measurements meaning that the surrounding environment of a molecule affects its ionisation behaviour much. Namely, some organic neutral molecules can be detected as $[M+K]^+$ with high sensitivity if they coexisted with K. In such cases, special attention should be paid to that the K distribution overlaps or being wider than the distribution of the target molecules or not. If the target molecule might be detected from the specific cell or tissue with or without K, the K-depending difference has to be discussed carefully. Similarly, Cl is an important element to measure negative ion spectra.

Regarding the distribution of inorganic elements, K is detected not only from cells and tissues having high physiological activity but also from dead cells and tissues in certain cases (Kuroda et al. 2013; Matsunaga et al. 2006; Metzner et al. 2008). Alkaline earth metals are also detectable in cryo-TOF-SIMS measurements with relatively lower sensitivity than that of alkaline metals, and their detection states were not $[M]^{2+}$ but $[M]^+$ (Zheng et al. 2017). Ca is detectable especially in the phloem region, and a specific salt crystalline (e.g., with oxalic acid) might be detected with strong intensity. Mg is also detectable in phloem region mainly. The ionisation tendency of these inorganic metals shows the similar hierarchy in both of dried and frozen-hydrated states.

Since the exact masses of inorganic elements are quite characteristic and easily distinguished from that of organics, the visualization certainty is high. Furthermore, the isotope labelling technique is useful to conduct tracer experiments. The *in planta* transfer behaviour of an essential element K (Metzner et al. 2008), a pollutive element Cs (Aoki et al. 2017), and a media H_2O (Iijima et al. 2011) were studied using their stable isotopes. The detection of water cluster ions $[(H_2O)_n+H]^+$ is generally reported for cryo-TOF-SIMS measurements (Cannon et al. 2000; Colliver et al. 1997; Pacholski et al. 1998; Roddy et al. 2002). Those cluster ions are important in cryo-TOF-SIMS measurements because they can be used for the m/z calibration in the spectrum without any additives.

4.2 Standard spectra of organic compounds

Owing to its wide distribution and the strong matrix effect of K as described above, the authors generally use KCl aqueous solutions (aq.) of standard water-soluble compounds to obtain their standard cryo-TOF-SIMS spectra imitating their *in planta* chemical environments. Furthermore, to verify the ionisation behaviours of target compounds in plants, the standard compounds were added to the aqueous plant extract, frozen, and measured by cryo-TOF-SIMS (Aoki et al. 2016). As a result, the enhanced secondary ion species agreed with those detected in spectra obtained using standard compounds dissolved in KClaq. Therefore, the authors believe that their ionisation behaviours are not so different within aqueous plant extract and KClaq.

In the cases of water-insoluble compounds, solutions of organic solvent such as acetone or hexane are available to prepare pseudo-hydrated and frozen standard samples by dropping the solution on a KClaq. base and then evaporating the organic solvents. In the cases of stilbenes, (+)-catechin, and abietic acid, they are detected without K-addition (Jyske et al. 2016, 2020), coniferyl alcohol and sinapyl alcohol are detected as K-added state to some extent (see below). Possibly the ratio of the derived secondary ion species varies depending on the matrix effect, and the situation that a molecule can be detected as several m/z values makes it difficult to obtain clear distribution images. The actual molecular-scale chemical environments in plants might be variable in plant cells and are not clarified in detail. Continuous research is needed to construct frozen-hydrated standard spectral database for an advanced biological and physiological discussions.

4.3 Saccharides and monolignols

Neutral hydrophilic compounds such as mono-/disaccharides are tends to be detected as potassium adduct ions of $[M+K]^+$ if they were frozen and measured as a solution in KClaq. as summarized in Figure 3. Hexoses ($C_6H_{12}O_6$) and sucrose ($C_{12}H_{22}O_{11}$) are detected as $[M+K]^+$ of m/z 219 and 381 ions, respectively (Aoki et al. 2016). In the cases of slightly acidic compounds of coniferyl alcohol and sinapyl alcohol, $[M\text{-}OH]^+$, $[M]^+$, $[M\text{-}H+K]^+$, and $[M+K]^+$ are detectable (Okumura et al. 2017), although their actual

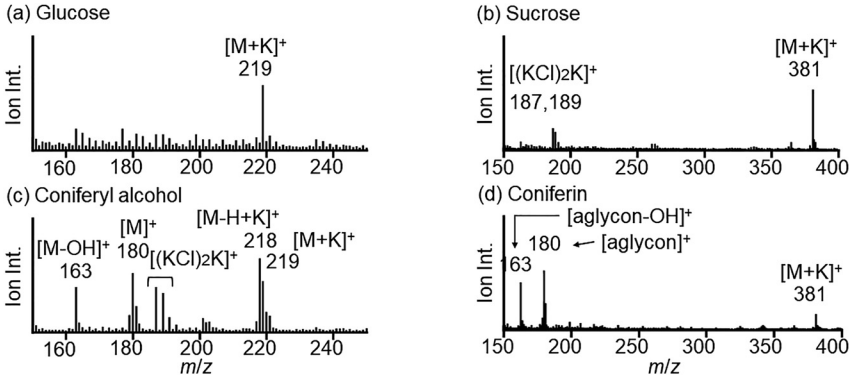

Figure 3: Cryo-TOF-SIMS spectra of (a) glucose, (b) sucrose, (c) coniferyl alcohol, and (d) coniferin frozen in KClaq.

amounts in some examined plant samples (stems of *Ginkgo biloba* L. and *Syringa vulgaris* L.) were quite small.

Monolignol glucosides consist of a monolignol and a glucose. Coniferyl alcohol ($C_{10}H_{12}O_3$) and sinapyl alcohol ($C_{11}H_{14}O_4$) are glucosylated ($+C_6H_{10}O_5$) and called as coniferin ($C_{16}H_{22}O_8$) and syringin ($C_{17}H_{24}O_9$), respectively. Coniferin and syringin are detectable as $[M+K]^+$ ions (Aoki et al. 2016, 2019; Okumura et al. 2017), and a serious mass overlapping arises here. That is coniferin ($[M+K]^+$, exact mass 381.0946) and sucrose ($[M+K]^+$, exact mass 381.0794) have very similar masses. To visualize them independently, apparatus having tandem MS system or very high mass resolution should be needed. Fortunately, their fragmentation behaviours were different. Sucrose in KClaq. does not produce *m*/*z* 180 ion as its fragment ion, and an aglycon fragment ion of *m*/*z* 180 can be used for the coniferin visualization (Aoki et al. 2016). Here, the origin of the *m*/*z* 180 ion was determined as the coniferyl alcohol unit of coniferin by ^{13}C labelling experiments.

On the other hand, there was no specific molecular or fragment ion derived only from sucrose and it is still a subject to visualize sucrose independently with high reliability, although the actual storage amount of sucrose is high and the *m*/*z* 381 ion should reflect the sucrose distribution mainly. One possible approach should be the high mass resolution apparatus to separate their mass difference. Similarly, the isomeric compounds such as hexoses, pentoses, and disaccharides having the same mass cannot be distinguished only by TOF-SIMS measurements at present.

The representative distributions of K, phosphatidylcholine, hexoses (glucose and fructose), sucrose, and coniferin in stems of *G. biloba* are displayed in Figure 4 with the total ion and cryo-SEM images (Aoki et al. 2016, 2018). The image shows the region containing phloem, cambial zone, differentiating xylem, and mature xylem. K and phosphatidylcholine derived ions are detected mainly from living cells. Hexoses, coniferin, and sucrose distributed differently. These distributions were roughly

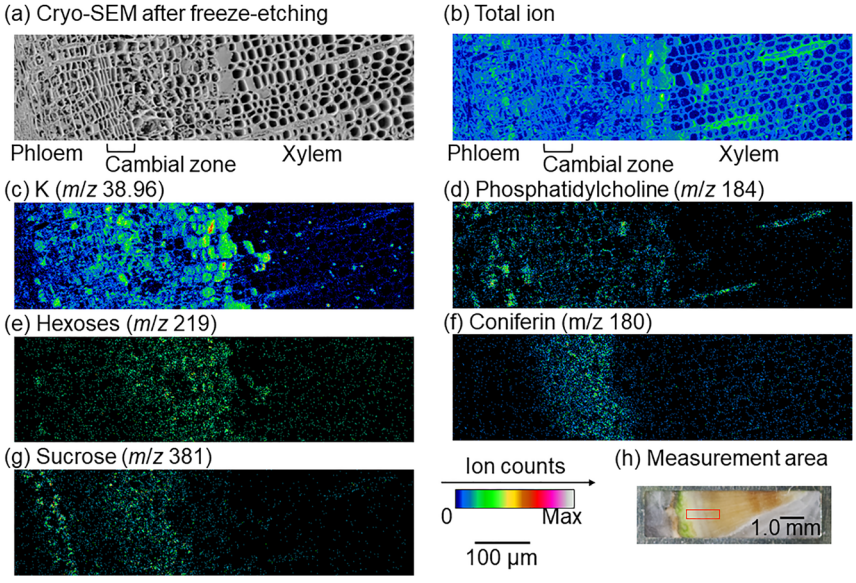

Figure 4: Visualization of several components in freeze-fixed stem of *Gingko biloba* by cryo-TOF-SIMS/SEM measurement: (a) cryo-SEM after freeze-etching and cryo-TOF-SIMS images for (b) total ion, (c) K, (d) phosphatidylcholine, (e) hexoses (mainly glucose and fructose), (f) coniferin, and (g) sucrose. Measurement area of the frozen sample was shown in (h).

confirmed by chromatography quantifications using the serial tangential sections (100 μm thickness) of the ginkgo stem as schematically illustrated in Figure 2b.

Monolignol glucosides are a promising candidate of storage and transport forms of monolignols as a lignin precursor (Dharmawardhana et al. 1995; Samuels et al. 2002; Terashima et al. 2016; Whetten et al. 1998). It has been reported that several wood species store coniferin around cambial zones (Fukushima et al. 1996, 1997; Savidge 1989; Terazawa et al. 1984; Tsuyama and Takabe 2014) and some of imaging chemical analyses examined the situation using freeze-dried section samples (Morikawa et al. 2010; Yoshinaga et al. 2015). By the cryo-TOF-SIMS measurements of freeze-fixed stem of *G. biloba*, it is clearly visualized that coniferin is stored in tracheid cells from the cambial zone to the differentiating xylem region and diminished at the cells in the secondary wall bulk lignification stage as determined by microscopic observations using visible, polarized, and UV lights as indicated in Figure 2b.

TOF-SIMS can visualize the actual amount at the position and does not indicate the biosynthesis activity of the target compounds on there. Therefore, the resultant image suggests the difference between the biosynthesis and the consumption. . Cellular distribution of coniferin showed good agreement with the assimilation timing of coniferin to lignin in differentiating xylem region previously visualized by ^{14}C-labelled coniferin administration experiments (Fukushima and Terashima 1991). From these results, the authors concluded that coniferin is stored in the tracheid cells of differentiating xylem and is utilised as a lignin precursor in ginkgo stem.

4.4 Ionic compounds and complex

As for the detection sensitivity, it is generally accepted that the secondary ion yield for organic compounds in usual TOF-SIMS measurements are lower than 1% (Piwowar and Vickerman 2010; Van der Heide 2014b; Vickerman 2001). In the case of sucrose as $[M+K]^+$ ion, the detectability is improved and sucrose can be visualized with good sensitivity. Furthermore, if the target molecule was ionic in nature, the detectability can be much better. With a simple calculation using the actual molar amount and secondary ion counts, for example, the detection sensitivity of salicifoline (quaternary ammonium alkaloid, $C_{12}H_{20}NO_2$, detected as $[M]^+$) was stronger than that of sucrose (detected as $[M+K]^+$) for a several hundred times (Okumura et al. 2017).

In this point, tertiary and quaternary nitrogen containing molecules may show good ionisation efficiency because of its elemental character. One typical secondary ion detectable in plants is the phosphocholine fragment ion ($[C_5H_{15}NO_4P]^+$, m/z 184.07) (Cannon et al. 2000; Cliff et al. 2003; Roddy et al. 2002) derived from phosphatidylcholine which is the major component of the plant biological membranes (Khan and Williams 1977). On the other hand, a primary amine compound such as cadaverine ($C_5H_{14}N_2$, detected as $[M+H]^+$) did not show such a high detectability (Oota et al. 2020).

Direct detection of an ionic complex is one of the latest achievements in cryo-TOF-SIMS applications. It is usually difficult to isolate the ionic complex as it was and prove its presence in the biological samples; therefore, for example, the details of the pigment molecules involved in the colour expression of various flowers and the related colouring mechanisms are still unclear (Yoshida et al. 2021a, 2021b). Recently, the chemical structure of the blue pigment of *Hydrangea macrophylla* is proposed as a three-component ion complex consists of 3-*O*-glucosyl delphinidin, 5-*O*-caffeoylquinic acid, and Al^{3+} (Ito et al. 2018). This hydrangea-blue-complex (HBC) was detected by cryo-TOF-SIMS directly (Ito et al. 2019). As displayed in Figure 5, HBC was detected from the blue coloured cells in the hydrangea sepal and Al^+ was also detected from the same regions. Interestingly, co-pigments (5-*O*-caffeoylquinic acid and 3-*O*-caffeoylquinic acid) were significantly detected from the neighbouring surface epidermal cells. Their molecular mechanisms capturing and detoxifying the Al ion are still a hot issue.

4.5 Hydrophobic compounds

Similar to the examples of the water-soluble compounds described above, even the hydrophobic compounds are also mobile or dispersive. That is, the distribution information deteriorates through processes such as drying, chemical fixation, solvent exchange, etc. For lipid compounds, the migration possibility was recognized earlier and some of cryo-experiments were reported as effective technique to stop their diffusion using model systems, unicellular organisms, and animal tissues (Cannon et al. 2000; Newell et al. 2019; Phan et al. 2014; Piehowski et al. 2008; Sämfors et al. 2019; Sjövall et al. 2006; Zhang et al. 2020).

For the cases of plants, a phospholipid fragment of m/z 184 ion was previously introduced. As a different type of lipid, it is well known that there are much amount of fatty

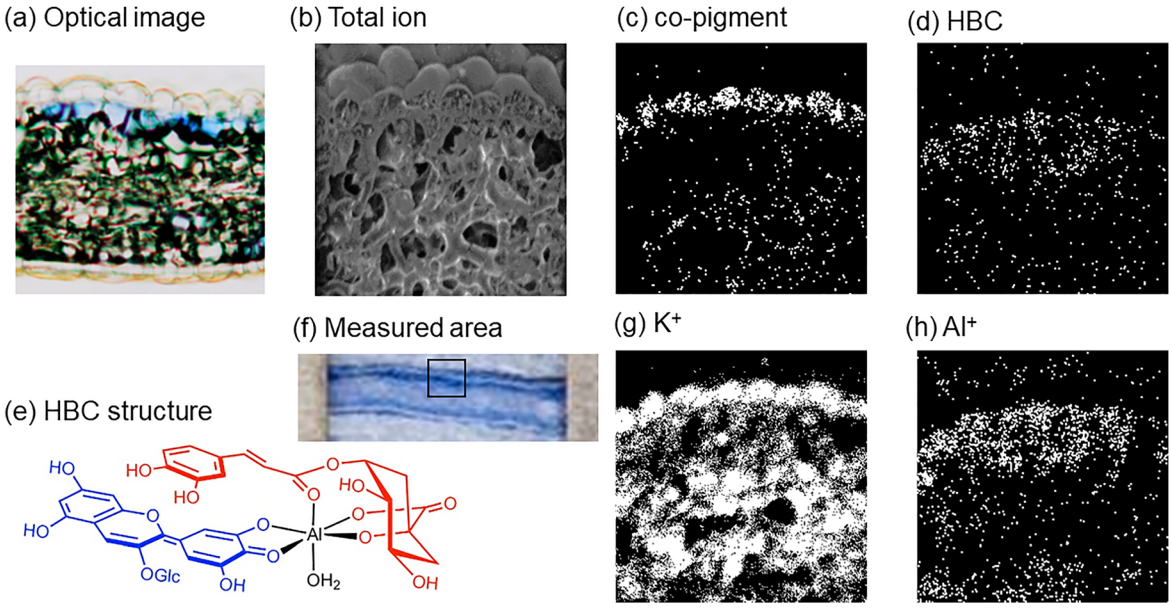

Figure 5: Hydrangea blue complex in the blue-coloured cells with Al, detected by cryo-TOF-SIMS.

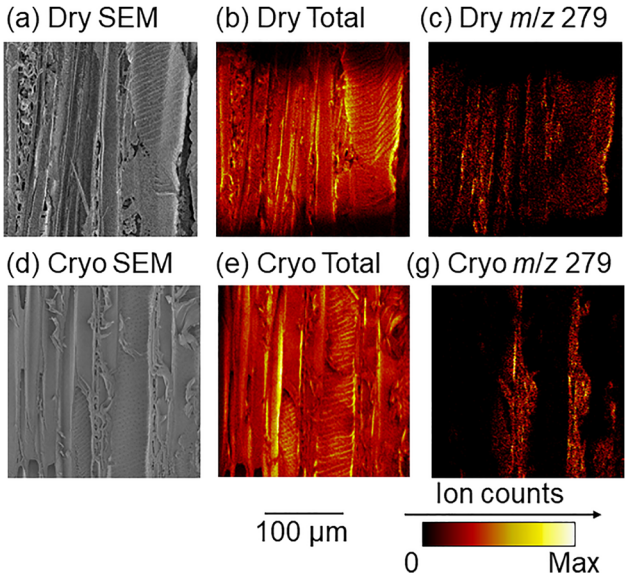

Figure 6: Fatty acid distribution in (a, b, c) dried or (d, e, f) freeze-fixed stems of *Tilia japonica*. Images by (a, d) cryo-SEM, (b, e) TOF-SIMS total ion, and (c, f) TOF-SIMS *m/z* 279 ion (linoleic acid).

acids in plants (Post-Beittenmiller 1996; Tupper-Carry and Priestley 1923). Fatty acid is easily detectable in negative-ion mode as $[M–H]^-$ ion derived from free fatty acid or corresponding glycerol esters (Hearn and Briggs 1991; Kleen et al. 2003). Long chain fatty acids and their esters have relatively higher molecular weights; however, their melting points are often lower than room temperature especially for ones having unsaturated bonds (Thomas et al. 2015).

Recently, lipid behaviours in woody plants are studied to discuss the role of intervessel pit membranes (Yamagishi et al. 2021). Typical and conventional images about fatty acids in wood are displayed in Figure 6a–c. As a result of room temperature storage, drying, or any other artificial effect, they distributed to wide area. However, if the sample was freeze-fixed and measured as the frozen-hydrated state, the fatty acids are localized only to the parenchyma regions as visualized in Figure 6d–f. This result clearly shows the freeze-fixation importance to discuss the *in planta* role of mobile or dispersive molecules considering their distributions.

4.6 Artificial reagents in aqueous reaction systems

The freeze-fixation technique is a good approach to visualize the intermediate state of the target reactions or processes. The aqueous heterogeneous systems of papermaking (Masumi et al. 2014) and pulping (Tokugawa et al. 2017) processes were studied using cryo-TOF-SIMS. A cationic polymer additive is used in the papermaking process as a retention aid, it holds small particles containing fine fibres, and increases the paper yield. By cryo-TOF-SIMS measurements of a frozen wet hand-sheet sample, the cationic polymer of poly(dimethyl-diallylammonium chloride) (PDADMAC) was detected on the fibre surfaces unevenly and not detected at the transverse sections of the pulp fibre (Masumi et al. 2014). Especially PDADMAC was

detected on the tangled fibrils located between the fibres. This result clearly demonstrates the expected roles of PDADMAC as a retention aid.

On the other hand, a nonionic polymer can be used as a detergent after the wood chip digesting process. After a kraft digestion of wood chips, the resultant pulp was washed with water containing the nonionic polymer of polyoxyalkylene alkyl ether (POA), frozen, and measured by cryo-TOF-SIMS (Tokugawa et al. 2017). In the view field, there were several circular transverse sections of the pulp fibres, and POA distributed in the washing water and the lumen region of the pulp fibres. Further, POA was detected at the transverse sections of the pulp stronger than at the washing water region. This result suggests that POA easily permeate into the pulp fibres (cell walls) and may accelerate the solution exchanging processes and play the detergent role. These different behaviours of cationic and nonionic polymer additives in pulp and papermaking processes are expected earlier as a matter of course; nevertheless, the visualized scenes give us new insights into their molecular mechanisms and should lead further developments.

A different type of reaction was examined by cryo-TOF-SIMS. The solute diffusion into cell walls in solution-impregnated wood block samples was successfully visualized (Zheng et al. 2018). The diffusion processes of melamine formaldehyde solution can be controlled by the environmental relative humidity and the conditioning processes was examined in detail.

5 Concluding remarks

The spatial resolution of the latest TOF-SIMS apparatuses is better than 100 nm and enough to discuss intracellular organelles such as a nucleus, a Golgi, a mitochondria, a chloroplast, etc.; however, the higher microscopic resolution is achieved, the finer and careful sample surface preparation techniques is needed. Furthermore, the theoretical limit of the freeze-fixation technique is apparent, that is the animation impossibility. In contrast to this point, the frozen sample can be measured for a long time with appropriate storage conditions and the frozen sample can also be transferred to another measurement apparatus operated in the different building. Still yet there is no method detecting and visualizing all types of molecules in biological samples at the same time, the authors hope some of them can be examined by cryo-TOF-SIMS and useful information for the future discussion can be provided.

Acknowledgements: The authors thank K. Kuroda, Forestry and Forest Products Research Institute, and R. Takama, Nagoya University, for their help with the cryo-TOF-SIMS system operation.

Author contributions: All the authors have accepted responsibility for the entire content of this submitted manuscript and approved submission.

Research funding: This study was financially supported by the Japan Society for the Promotion of Science KAKENHI (nos. 212280004, 22580188, 25110507, 25114508, 25252032, 15H00975, 15H01230, 18H03959).

Conflict of interest statement: The authors declare no conflicts of interest regarding this article.

References

Aoki, D., Asai, R., Tomioka, R., Matsushita, Y., Asakura, H., Tabuchi, M., and Fukushima, K. (2017). Translocation of ^{133}Cs administered to *Cryptomeria japonica* wood. Sci. Total Environ. 584–585: 88–95.

Aoki, D., Hanaya, Y., Akita, A., Matsushita, Y., Yoshida, M., Kuroda, K., Yagami, S., Takama, R., and Fukushima, K. (2016). Distribution of coniferin in freeze-fixed stem of *Ginkgo biloba* L. by cryo-TOF-SIMS/SEM. Sci. Rep. 6: 31525.

Aoki, D., Matsushita, Y., and Fukushima, K. (2018). Cryo-TOF-SIMS visualization of water-soluble compounds in plants. In: Jayaprakasha, G.K., Patil, B.S., and Gattuso, G. (Eds.), *Advances in plant phenolics: from chemistry to human health*. ACS Symposium Series. American Chemical Society, Washington, DC, pp. 137–150.

Aoki, D., Okumura, W., Akita, T., Matsushita, Y., Yoshida, M., Sano, Y., and Fukushima, K. (2019). Microscopic distribution of syringin in freeze-fixed *Syringa vulgaris* stems. Plant Direct 3: 1–8.

Bernius, M.T., Chandra, S., and Morrison, G.H. (1985). Cryogenic sample stage for the Cameca IMS3f ion microscope. Rev. Sci. Instrum. 56: 1347–1351.

Cannon, D.M., Pacholski, M.L., Winograd, N., and Ewing, A.G. (2000). Molecule specific imaging of freeze-fractured, frozen-hydrated model membrane systems using mass spectrometry. J. Am. Chem. Soc. 122: 603–610.

Chandra, S., Bernius, M.T., and Morrison, G.H. (1986). Intracellular localization of diffusible elements in frozen-hydrated biological specimens with ion microscopy. Anal. Chem. 1986: 493–496.

Cliff, B., Lockyer, N.P., Corlett, C., and Vickerman, J.C. (2003). Development of instrumentation for routine ToF-SIMS imaging analysis of biological material. Appl. Surf. Sci. 203–204: 730–733.

Colliver, T.L., Brummel, C.L., Pacholski, M.L., Swanek, F.D., Ewing, A.G., and Winograd, N. (1997). Atomic and molecular imaging at the single-cell level with TOF-SIMS. Anal. Chem. 69: 2225–2231.

Delcorte, A. (2001). Fundamental aspects of organic SIMS. In: Vickerman, J.C. and Briggs, D. (Eds.), *TOF-SIMS: surface analysis by mass spectrometry*. IM Publications and Surface Spectra Ltd., Manchester, pp. 161–194.

Dharmawardhana, D.P., Ellis, B.E., and Carson, J.E. (1995). A β-glucosidase from lodgepole pine xylem specific for the lignin precursor coniferin. Plant Physiol. 107: 331–339.

Fisher, G.L., Buinen, A.L., Potočnik, N.O., Hammond, J.S., Bryan, S.R., Larson, P.E., and Heeren, R.M.A. (2016). A new method and mass spectrometer design for TOF-SIMS parallel imaging MS/MS. Anal. Chem. 88: 6433–6440.

Fukushima, K., Taguchi, S., Matsui, N., and Yasuda, S. (1996). Heterogeneous distribution of monolignol glucosides in the stems of *Magnolia kobus*. Mokuzai Gakkaishi 42: 1029–1031.

Fukushima, K., Taguchi, S., Matsui, N., and Yasuda, S. (1997). Distribution and seasonal changes of monolignol glucosides in *Pinus thunbergii*. Mokuzai Gakkaishi 43: 254–259.

Fukushima, K. and Terashima, N. (1991). Heterogeneity in formation of lignin XIV. Formation and structure of lignin in differentiating xylem of *Ginkgo biloba*. Holzforschung 45: 87–94.

Goacher, R.E., Jeremic, D., and Master, E.R. (2011). Expanding the library of secondary ions that distinguish lignin and polysaccharides in time-of-flight secondary ion mass spectrometry analysis of wood. Anal. Chem. 83: 804–812.

Hagenhoff, B. (2001). Optimisation methods: cationisation. In: Vickerman, J.C. and Briggs, D. (Eds.), *TOF-SIMS: surface analysis by mass spectrometry*. IM Publications and Surface Spectra Ltd., Manchester, pp. 285–308.

Hearn, M.J. and Briggs, D. (1991). TOF-SIMS studies of carbon-fibre surfaces and carbon-fibre composite fracture surfaces. Surf. Interface Anal. 17: 421–429.

Iijima, M., Yoshida, T., Kato, T., Kawasaki, M., Watanabe, T., and Somasundaram, S. (2011). Visualization of lateral water transport pathways in soybean by a time of flight-secondary ion mass spectrometry cryo-system. J. Exp. Bot. 62: 2179–2188.

Ito, T., Oyama, K., and Yoshida, K. (2018). Direct observation of hydrangea blue-complex composed of 3-*O*-glucosyldelphinidin, Al^{3+} and 5-*O*-acylquinic acid by ESI-mass spectrometry. Molecules 23: 1424.

Ito, T., Aoki, D., Fukushima, K., and Yoshida, K. (2019). Direct mapping of hydrangea blue-complex in sepal tissues of *Hydrangea macrophylla*. Sci. Rep. 9: 5450.

Jyske, T., Kuroda, K., Keriö, S., Pranovich, A., Linnakoski, R., Hayashi, N., Aoki, D., and Fukushima, K. (2020). Localization of (+)-catechin in *Picea abies* phloem: responses to wounding and fungal inoculation. Molecules 25: 2952.

Jyske, T., Kuroda, K., Suuronen, J.-P., Pranovich, A., Roig-Juan, S., Aoki, D., and Fukushima, K. (2016). In planta localization of stilbenes within *Picea abies* Phloem. Plant Physiol. 172: 913–928.

Khan, M.-U. and Williams, J. P. (1977). Improved thin-layer chromatographic method for the separation of major phospholipids and glycolipids from plant lipid extracts and phosphatidyl glycerol and bis(monoacylglyceryl) phosphate from animal lipid extracts. J. Chromatogr. 140: 179–185.

Kirkby, E. (2012). Introduction, definition and classification of nutrients. In: Marschner, H. (Ed.), *Marschner's mineral nutrition of higher plants*, 3rd ed. Academic Press, Amsterdam, pp. 3–5.

Kleen, M., Kangas, H., and Laine, C. (2003). Chemical characterization of mechanical pulp fines and fiber surface layers. Nord. Pulp Paper Res. 18: 412003.

Kuroda, K., Fujiwara, T., Imai, T., Takama, R., Saito, K., Matsushita, Y., and Fukushima, K. (2013). The cryo-TOF-SIMS/SEM system for the analysis of the chemical distribution in freeze-fixed *Cryptomeria japonica* wood. Surf. Interface Anal. 45: 215–219.

Lancelle, S., Callaham, D.A., and Hepler, P.K. (1986). A method for rapid freeze fixation of plant cells. Protoplasma 131: 153–165.

Masumi, T., Matsushita, Y., Aoki, D., Takama, R., Saito, K., Kuroda, K., and Fukushima, K. (2014). Adsorption behavior of poly(dimethyldiallylammonium chloride) on pulp fiber studied by cryo time-of-flight secondary ion mass spectrometry and cryo-scanning electron microscopy. Appl. Surf. Sci. 289: 155–159.

Matsunaga, H., Shiotari, R., Matsumura, J., Oda, K., Utsumi, Y., and Yamamoto, K. (2006). Potassium distribution in black heartwood of sugi (*Cryptomeria japonica*) I: localization in axial parenchyma cells. J. Wood Sci. 52: 95–100.

Metzner, R., Schneider, H.U., Breuer, U., and Schoroeder, W.H. (2008). Imaging nutrient distributions in plant tissue using time-of-flight secondary ion mass spectrometry and scanning electron microscopy. Plant Physiol. 147: 1774–1787.

Möller, J., Beumer, A., Lipinsky, D., and Arlinghaus, H.F. (2006). Introduction of a cryosectioning-ToF-SIMS instrument for analysis of non-dehydrated biological samples. Appl. Surf. Sci. 252: 6709–6711.

Morikawa, Y., Yoshinaga, A., Kamitakahara, H., Wada, M., and Takabe, K. (2010). Cellular distribution of coniferin in differentiating xylem of *Chamaecyparis obtusa* as revealed by Raman microscopy. Holzforschung 64: 61–67.

Newell, C.L., Vorng, J.-L., MacRae, J.I., Gilmore, I.S., and Gould, A.P. (2019). Cryogenic OrbiSIMS localizes semi-volatile molecules in biological tissues. Angew. Chem. Int. Ed. 59: 18194–18200.

Okumura, W., Aoki, D., Matsushita, Y., Yoshida, M., and Fukushima, K. (2017). Distribution of salicifoline in freeze-fixed stems of *Magnolia kobus* as observed by cryo-TOF-SIMS. Sci. Rep. 7: 5939.

Oota, M., Tsai, A.Y.-L., Aoki, D., Matsushita, Y., Toyoda, S., Fukushima, K., Saeki, K., Toda, K., Perfus-Barbeoch, L., Favery, B., et al. (2020). Identification of naturally occurring polyamines as root-knot nematode attractants. Mol. Plant 13: 658–665.

Pacholski, M.L., Cannon, D.M., Jr., Ewing, A.G., and Winograd, N. (1998). Static time-of-flight secondary ion mass spectrometry imaging of freeze-fractured, frozen-hydrated biological membranes. Rapid Commun. Mass Spectrom. 12: 1232–1235.

Passarelli, M., Pirkl, A., Moellers, R., Grinfeld, D., Kollmer, F., Havelund, R., Newman, C.F., Marshall, P.S., Arlinghaus, H., Alexander, M.R., et al. (2017). The 3D OrbiSIMS—label-free metabolic imaging with subcellular lateral resolution and high mass-resolving power. Nat. Methods 14: 1175–1183.

Phan, N.T.N., Fletcher, J.S., Sjövall, P., and Ewing, A.G. (2014). ToF-SIMS imaging of lipids and lipid related compounds in Drosophila brain. Surf. Interface Anal. 46: 123–126.

Piehowski, P.D., Kurczy, M.E., Willingham, D., Parry, S., Heien, M.L., Winograd, N., and Ewing, A.G. (2008). Freeze-etching and vapor matrix deposition for ToF-SIMS imaging of single cells. Langmuir 24: 7906–7911.

Piwowar, A.M., Lockyer, N.P., and Vickerman, J.C. (2009). Salt effects on ion formation in desorption mass spectrometry: an investigation into the role of alkali chlorides on peak suppression in time-of-flight-secondary ion mass spectrometry. Anal. Chem. 81: 1040–1048.

Piwowar, A.M. and Vickerman, J.C. (2010). The role of molecular weight on the ToF-SIMS spectra of PMMA using Au^+ and C_{60}^+ primary ions. Surf. Interface Anal. 42: 1387–1392.

Post-Beittenmiller, D. (1996). Biochemistry and molecular biology of wax production in plants. Annu. Rev. Plant Physiol. Plant Mol. Biol. 47: 405–430.

Roddy, T.P., Cannon, D.M., Jr., Ostrowski, S.G., Winograd, N., and Ewing, A.G. (2002). Identification of cellular sections with imaging mass spectrometry following freeze fracture. Anal. Chem. 74: 4020–4026.

Saito, K., Kato, T., Tsuji, Y., and Fukushima, K. (2005a). Identifying the characteristic secondary ions of lignin polymer using ToF-SIMS. Biomacromolecules 6: 678–683.

Saito, K., Kato, T., Takamori, H., Kishimoto, T., and Fukushima, K. (2005b). A new analysis of the depolymerized fragments of lignin polymer using ToF-SIMS. Biomacromolecules 6: 2688–2696.

Saito, K., Kato, T., Takamori, H., Kishimoto, T., Yamamoto, A., and Fukushima, K. (2006). A new analysis of the depolymerized fragments of lignin polymer in the plant cell walls using ToF-SIMS. Appl. Surf. Sci. 252: 6734–6737.

Sämfors, S., Ståhlman, M., Klevstig, M., Borén, J., and Fletcher, J.S. (2019). Localised lipid accumulation detected in infarcted mouse heart tissue using ToF-SIMS. Int. J. Mass Spectrom. 437: 77–86.

Samuels, A.L., Rensing, K.H., Douglas, C.J., Mansfield, S.D., Dharmawardhana, D.P., and Ellis, B.E. (2002). Cellular machinery of wood production: differentiation of secondary xylem in Pinus contort ava. latifolia. Planta 216: 72–82.

Savidge, R.A. (1989). Coniferin, a biochemical indicator of commitment to tracheid differentiation in conifers. Can. J. Bot. 67: 2663–2668.

Sjövall, P., Johnasson, B., and Lausmaa, J. (2006). Localization of lipids in freeze-dried mouse brain sections by imaging TOF-SIMS. Appl. Surf. Sci. 252: 6966–6974.

Terashima, N., Ko, C., Matsushita, Y., and Westermark, U. (2016). Monolignol glucosides as intermediate compounds in lignin biosynthesis. Revisiting the cell wall lignification and new ^{13}C-tracer experiments with Ginkgo biloba and *Magnolia liliiflora*. Holzforschung 70: 801–810.

Terazawa, M., Okuyama, H., and Miyake, M. (1984). Phenolic compounds in living tissue of woods I. Phenolic β-glucosides of 4-hydroxycinnamyl alcohol derivatives in the cambial sap of woods. Mokuzai Gakkaishi 30: 322–328.

Thomas, A., Matthäus, B., and Fiebig, H.-J. (2015). Fats and fatty oils 3.1 melting and freezing points. In: *Ullmann's Encyclopedia of industrial chemistry*. Wiley VCH, Weinheim, pp. 10–11.

Tokugawa, K., Aoki, D., Asai, R., Matsushita, Y., Ishiguro, M., Noda, Y., and Fukushima, K. (2017). Behavioural analysis of a nonionic detergent in the kraft pulp washing process using cryo-time-of-flight secondary ion mass spectrometry and cryo-scanning electron microscopy. J. Wood Sci. 63: 281–287.

Tsuyama, T. and Takabe, K. (2014). Distribution of lignin and lignin precursors in differentiating xylem of Japanese cypress and poplar. J. Wood Sci. 60: 353–361.

Tupper-Carry, R.M. and Priestley, J.H. (1923). The composition of the cell-wall at the apical meristem of stem and root. Proc. Royal Soc. B 95: 109–131.

Tyler, B.J., Rangaranjan, S., Möller, J., Beumer, A., and Arlinghaus, H.F. (2006). TOF-SIMS imaging of chlorhexidine-digluconate transport in frozen hydrated biofilms of the fungus *Candida albicans*. Appl. Surf. Sci. 252: 6712–6715.

Van der Heide, P. (2014a). The fundamentals of SIMS. In: *Secondary ion mass spectrometry: an introduction to principles and practices*. John Wiley & Sons, Inc., Hoboken, pp. 44–46.

Van der Heide, P. (2014b). Models of molecular secondary ions. In: *Secondary ion mass spectrometry: an introduction to principles and practices*. John Wiley & Sons, Inc., Hoboken, pp. 130–138.

Vickerman, J.C. (2001). ToF-SIMS—an overview. In: Vickerman, J.C. and Briggs, D. (Eds.), *TOF-SIMS: surface analysis by mass spectrometry*. IM Publications and Surface Spectra Ltd., Manchester, pp. 1–40.

Vickerman, J.C. (2011). Molecular imaging and depth profiling by mass spectrometry—SIMS, MALDI or DESI? Analyst 136: 2199–2177.

Whetten, R.W., MacKay, J.J., and Sederoff, R.R. (1998). Recent advances in understanding lignin biosynthesis. Annu. Rev. Plant Physiol. Plant Mol. Biol. 49: 585–609.

Yamagishi, S., Shigetomi, K., Fujiyasu, S., Aoki, D., Uno, T., Fukushima, K., and Sano, Y. (2021). Artifactual lipid coatings on intervessel pit membranes in dried xylem tissues of some angiosperms. IAWA J. 42: 365–383.

Yoon, S. and Lee, T.G. (2018). Biological tissue sample preparation for time-of-flight secondary ion mass spectrometry (ToF–SIMS) imaging. Nano Converg. 5: 24.

Yoshida, K., Ito, D., Miki, N., and Kondo, T. (2021a). Single-cell analysis clarifies mosaic color development in purple hydrangea sepal. New Phytol. 229: 3579–3557.

Yoshida, K., Oyama, K., and Kondo, T. (2021b). Insight into chemical mechanisms of sepal color development and variation in hydrangea. Proc. Jpn. Acad, Ser. B 97: 51–68.

Yoshinaga, A., Kamitakahara, H., and Takabe, K. (2015). Distribution of coniferin in differentiating normal and compression woods using MALDI mass spectrometric imaging coupled with osmium tetroxide vapor treatment. Tree Physiol. 36: 643–652.

Zhang, J., Brown, J., Scurr, D.J., Bullen, A., MacLellan-Gibson, K., Williams, P., Alexander, M.R., Hardie, K.R., Gilmore, I.S., and Rakowska, P.D. (2020). Cryo-OrbiSIMS for 3D molecular imaging of a bacterial biofilm in its native state. Anal. Chem. 92: 9008–9015.

Zheng, P., Ito, T., Aoki, D., Sato, S., Yoshida, M., Sano, Y., Matsushita, Y., Fukushima, K., and Yoshida, K. (2017). Determination of inorganic element distribution in the freeze-fixed stem of $Al_2(SO_4)_3$-treated *Hydrangea macrophylla* by TOF-SIMS and ICP-AES. Holzforschung 71: 471–480.

Zheng, P., Aoki, D., Seki, M., Miki, T., Tanaka, S., Kanayama, K., Matsushita, Y., and Fukushima, K. (2018). Visualization of solute diffusion into cell walls in solution-impregnated wood under varying relative humidity using time-of-flight secondary ion mass spectrometry. Sci. Rep. 8: 9819.